Supplementary material

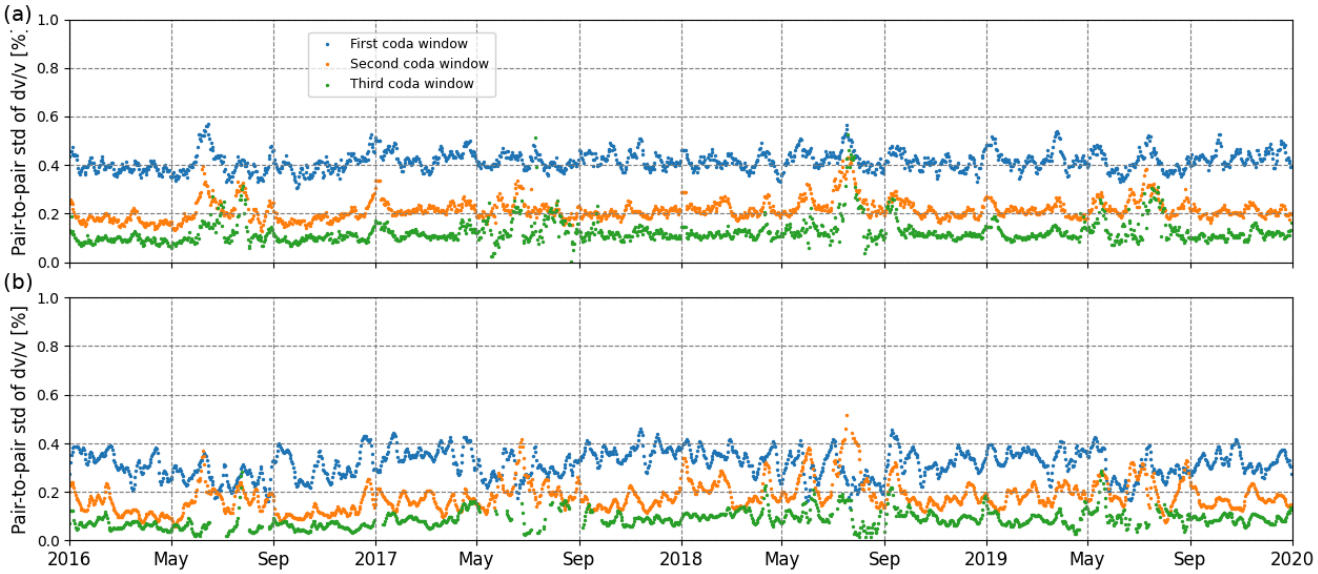

Figure S1. Pair-to-pair variability of the δv/v estimates for the full network and the path-selected subset. Daily standard deviation of δv/v values calculated across contributing station pairs for the three coda windows. Panel (a) shows results for all station pairs (N=190), and panel (b) shows results for the path-selected subset with interstation distance <20 km and azimuth 60^0-120^0 (N=23). The standard deviation represents pair-to-pair variability. The subset generally exhibits variability that is comparable to, and in many periods slightly lower than, that of the full network, while retaining a clearer seasonal mean signal.

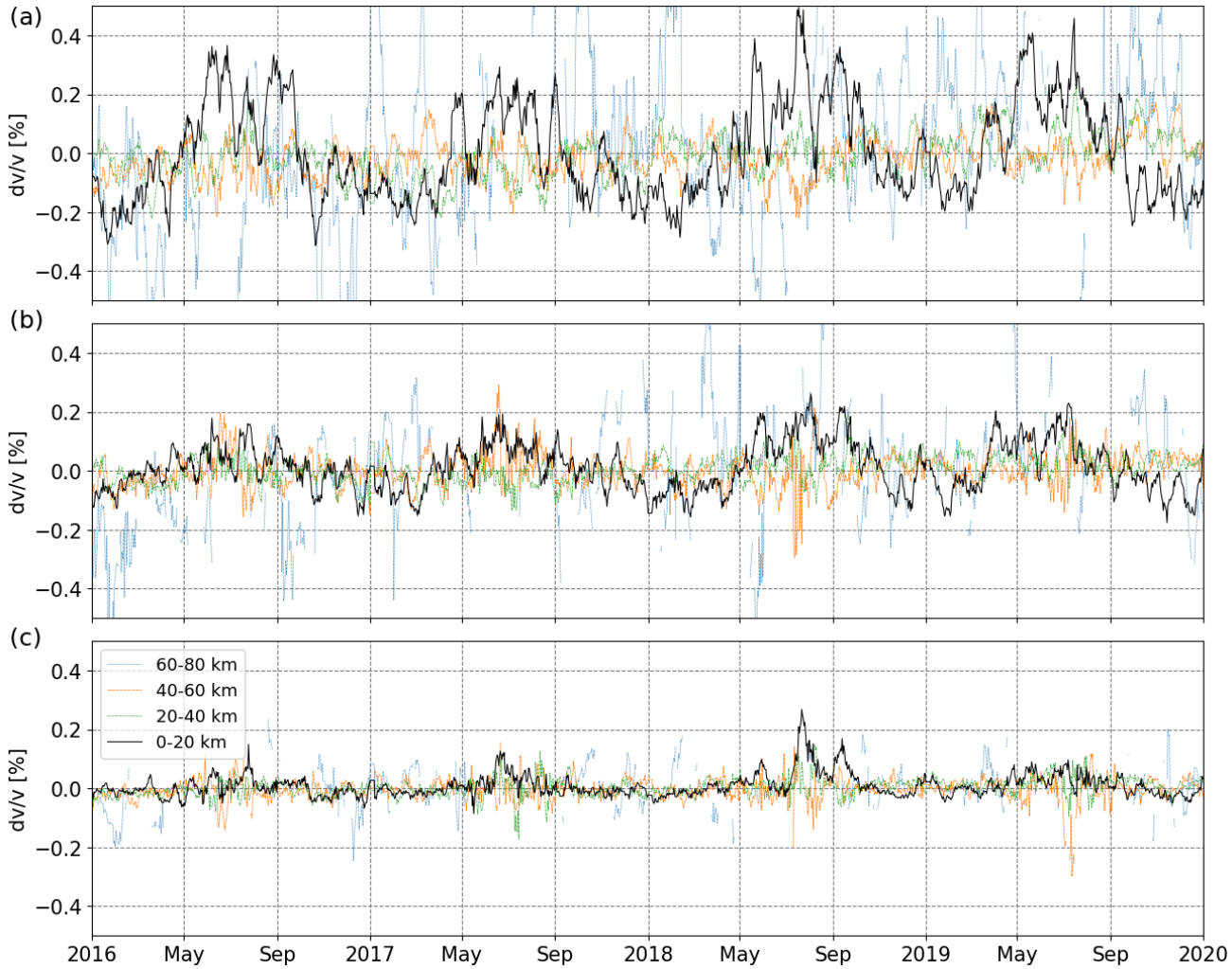

Figure S2. δv/v estimates for the entire region in the 0.1–0.5 Hz frequency band, computed using the first (a), second (b), and third (c) coda windows. The δv/v results are grouped by interstation distance. In each panel, δv/v result is highlighted for the pairs with interstation distance <20 km.

Figure S3. δv/v estimates for the entire region in the 0.1–0.5 Hz frequency band, computed using the first (a), second (b), and third (c) coda windows. The δv/v results are grouped by station-pair azimuth. In each panel, pairs with azimuths of 60–90° and 90–120° are highlighted with black and green lines, respectively.

Table S1. Robustness of the environmental correlations to station-pair subset selection of the W1 window. For each path selection, the table reports the number of station pairs, the strength or presence of the annual δv/v spectral peak, and the maximum lagged cross-correlation coefficients and corresponding lag times for temperature and groundwater level. Positive lag times indicate that δv/v lags the environmental variable. The selected subset with interstation distance <20 km and azimuth 60^0-120^0 gives the clearest seasonal signal, while nearby distance and azimuth selections show similar temperature-related correlations and lag times, indicating that the inferred dominant thermal control is not an artefact of a narrowly tuned subset. W1 is shown because it has the clearest seasonal signal; the same tests were also performed for W2 and W3 and showed similar temperature-lag behaviour, although with slightly weaker correlations.

Subset	No. of pairs	Annual PSD peak amplitude	Max corr. with temperature	Temperature lag (days)	Max corr. with groundwater	Groundwater lag (days)
All pairs	190	3.16	0.79	23	0.52	107
Distance < 20 km, all azimuths	65	28.38	0.92	19	0.56	108
All distances, azimuth 60^0-120^0	42	32.55	0.90	23	0.59	108
Distance < 20 km, azimuth 60^0-120^0	23	65.27	0.93	19	0.64	107
Distance < 25 km, azimuth 60^0-120^0	27	51.63	0.89	19	0.61	107
Distance < 20 km, azimuth 45^0-135^0	32	63.01	0.91	18	0.60	108

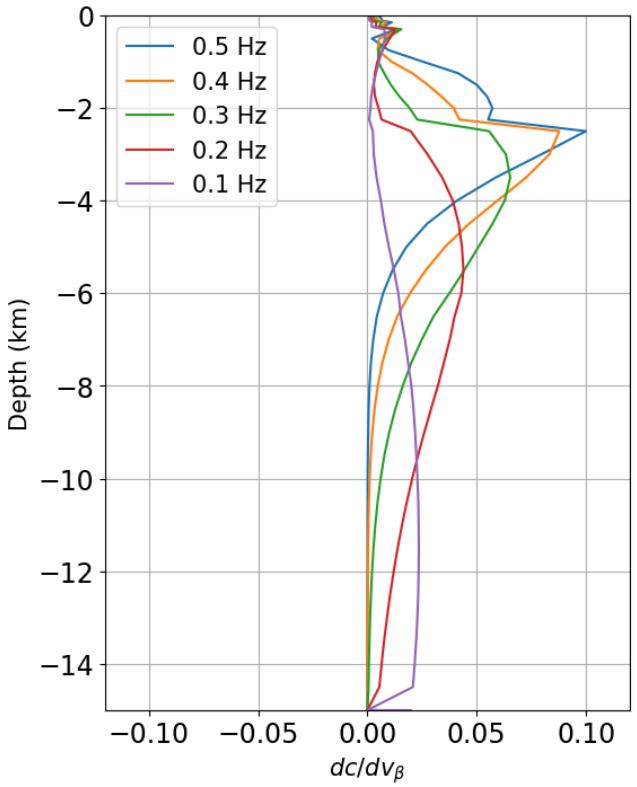

Figure S4. Rayleigh wave phase velocity sensitivity kernel for the study area for the frequency band 0.1-0.5 Hz using the velocity model by Malek et al. (2023) with the help of the Python program disba.

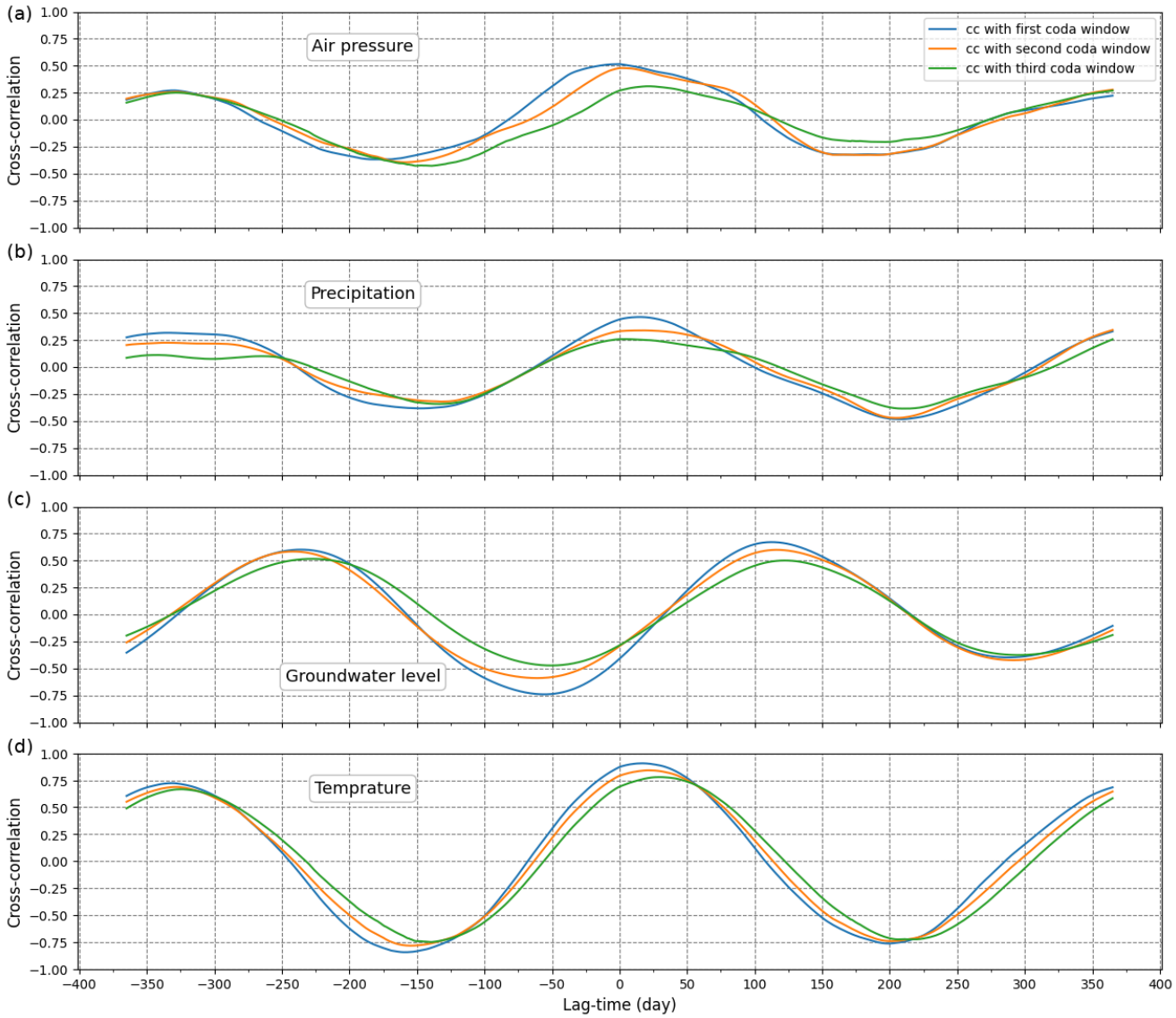

Figure S5. Cross-correlation estimates between δv/v and environmental variables after retaining periods longer than 100 days. Positive lag times indicate that δv/v lags the environmental signal.

References :

[1] Málek, J., Brokešová, J. & Novotný, O. New Velocity Structure of the Nový Kostel Earthquake-Swarm Region, West Bohemia, Determined by the Isometric Inversion. *Pure Appl. Geophys.* 180, 2111–2134 (2023). https://doi.org/10.1007/s00024-023-03250-w

[2] Luu, K. (2024). disba: Numba-accelerated computation of surface wave dispersion (v0.7.0). Zenodo. https://doi.org/10.5281/zenodo.14534395